EURASIAN PHYSICAL TECHNICAL JOURNAL

2026, Volume 23, No.1 (55)

https://doi.org/10.31489/2026

Received: 16/09/2025 Revised: 08/02/2026 Accepted: 19/03/2026 Published online: 30/03/2026

Original Research Article

UDC 536.8

PHYSICAL PROPERTIES OF A FREE-PISTON STIRLING ENGINE WITH A REVERSIBLE CHEMICAL REACTION OF DIOXSIDE NITROGEN ↔ TETRAOXSIDE NITROGEN IN THE WORKING GAS.

Sabdenov K.O., Konysbekova G.K.

L.N. Gumilyov Eurasian National University, Astana, Republic of Kazakhstan
*Corresponding author: gulbarshyn_1991@mail.ru

Abstract. *Simulation is used to study the properties of a free-piston Stirling engine in the isothermal approximation. The working substance is a chemically reacting gas mixture, in which mutual conversion of nitrogen dioxide and nitrogen tetroxide can occur in the reversible reaction* $2NO_2 \leftrightarrow N_2O_4$. *In the cooler, the exothermic reaction* $2NO_2 \rightarrow N_2O_4$ *occurs, in the heater at a high temperature, the endothermic reaction* $N_2O_4 \rightarrow 2NO_2$ *occurs. Two cases are compared: 1) the above chemical reaction occurs in the working gas, and 2) the working gas is chemically inert. The engine efficiency* η_{eng} *is higher in the first case over the range of heater temperature change from 90 to 130 ℃, and where* η_{eng} *increases from 0.345 to 0.383. In this case,* η_{eng} *turns out to be higher than that calculated using the Carnot formula with the same maximum and minimum temperatures. High efficiency is achieved thanks to the engine's ability to produce negative E. Schrödinger entropy.*

Keywords: free-piston Stirling engine, working gas with a reversible chemical reaction, nitrogen dioxide and nitrogen tetroxide.

1. Introduction

In recent scientific works [1-8] much attention has been paid to the production of mechanical work or electrical energy in thermodynamic systems with a reversible chemical reaction. The results of works [1, 2] predict the possibility of increasing the efficiency of thermodynamic cycles due to the reversible chemical reaction occurring in the working gas. In such cycles, under certain conditions, chemical work plays a significant role in the energy balance; it facilitates the conversion of heat into mechanical work. Using the properties of reversible chemical reactions to increase the efficiency of energy systems and production is not new. Substances where such reactions can occur are considered as energy accumulators in thermal power plants and other types of electricity production from low-potential heat sources [3-8]. Due to the reversibility of electrochemical reactions and thermodynamic cycles based on them, modern storage batteries exist [7, 8]. There are also earlier theoretical works [9-11] that show the possibility of creating Stirling engines with a reversible chemical reaction in the working gas and which will have a significantly higher efficiency than similar engines, but with a chemically inert working gas.

To achieve high efficiency in thermodynamic cycles with a reversible chemical reaction and a gas working substance, several conditions must be met [1, 2]:

– at the compression stage, the gas must have a high molecular weight, and at the expansion stage, a low one;

– the value of chemical work must be such as to completely or partially compensate for the heat release in the reverse chemical reaction in the cooler; this reduces the amount of heat released into the surrounding space;
– the temperatures of the heater and cooler should not differ greatly; this determines the condition for the existence of the cycle.

In [2], the analysis of the Stirling cycle with a reversible chemical reaction was carried out under the assumption of equilibrium processes in all four of its sections. Under the condition of the existence of a cycle, a reversible chemical reaction behaves as a periodic reaction, and the heat engine becomes similar to a biological object. In the simplest model, a chemical reaction is represented as a mutual transformation of two substances; the relative concentration of one of the substances g_A is added to the familiar thermodynamic parameters of pressure p, temperature T and specific volume υ. Then the cycle under consideration is depicted in three-dimensional space (Fig. 1, a), and it can be projected onto the well-known two-dimensional plane (Fig. 1, b). To analyze thermodynamic cycles with multicomponent reversible chemical reactions, it is necessary to move to a space of even higher dimensionality.

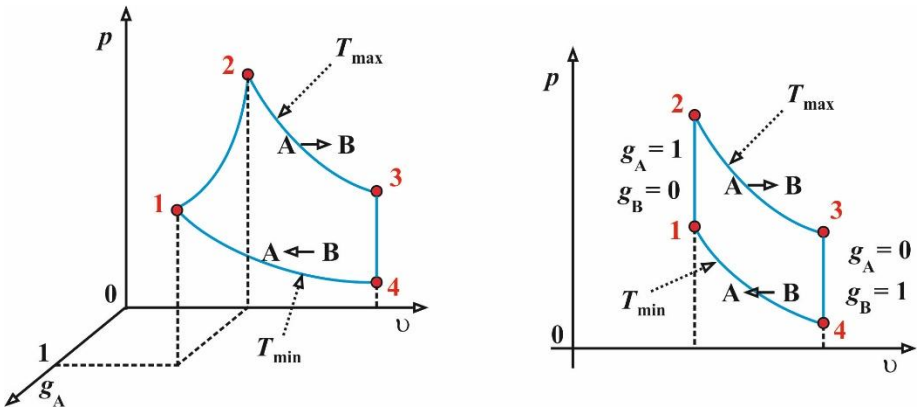

a) b)

Fig. 1. Ideal Stirling cycle with reversible chemical reaction A ↔ B (a) in three-dimensional space of variables p-υ-g_A and its projection onto the p-υ plane (b).

Such consideration of cycles in a multidimensional space of variables allows us to better understand the thermodynamic properties of heat engines with reversible chemical reactions; for example, in [7, 8] it is proposed to use the coordinates of temperature T, entropy S and Gibbs free energy G; the convenience of using the Gibbs energy as the third coordinate is manifested in its direct dependence on the concentration g_A.

According to the results of studies [1, 2], under certain conditions the efficiency of a heat engine can approach 1, and this indicates the possibility of creating better methods for producing electricity, especially from low-potential heat sources. Such theoretical conclusions need to be verified on physical experimental devices or on their virtual computer models. In this paper, the second method, also known as a computational experiment, is chosen. In particular, the operation of a Stirling engine with a free working piston is studied on the basis of a computer model. Its first mathematical model in the isothermal approximation was proposed in [12] and has since become the basis for many theoretical and experimental studies [13-18]. The isothermal approximation means accepting the assumption of a constant working gas temperature in the heater and cooler. The general name "Stirling engine" unites a wide class of mechanical devices operating on the basis of the thermodynamic Stirling cycle [18, 19]. Their mathematical models are represented by several differential equations, and they have (or should have) periodic solutions only when one parameter is not equal to one, and such a parameter is the ratio of the maximum temperature T_{max} (heater) to the minimum temperature T_{min} (cooler) $\Theta = T_{max}/T_{min}$ The models are also characterized by other physical and/or parameters, and may not have periodic solutions when $\Theta \neq 1$. But the fulfillment of this inequality is mandatory for the existence of periodic solutions.

The aim of this work is to search for and identify opportunities to achieve high efficiency in a Stirling engine with a reversible chemical reaction in the working gas $2NO_2 \leftrightarrow N_2O_4$. For this purpose, it is necessary at the first stage to conduct a simulation of the operation of a β-type engine, which will allow us to verify the main theoretical results of earlier studies [2, 9, 11].

2. Engine design diagram

The general design of the Stirling engine is shown in Fig. 2, where cooler 6 is the compression volume V_c, and heater 7 is the expansion volume V_e. In volumes V_c and V_e, constant values of temperature T_c and T_e are maintained. They are taken as the minimum and maximum temperature in the engine. The masses of gas in each of the specified volumes are equal to m_c and m_e, respectively. The mass exchange is performed at the rate of mass change in the regenerator m'_r, it is equal to the rates of mass change in the cooler $m'_c = m'_r$ and the heater $m'_c = m'_r$.

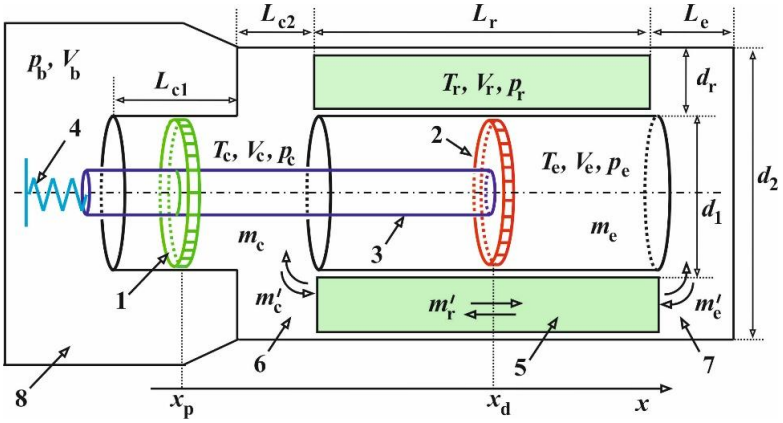

Fig. 2. Simplified diagram of a Stirling engine with a free piston; 1 – working piston; 2 – displacer; 3 – displacer rod; 4 – spring; 5 – regenerator; 6 – cooler; 7 – heater; 8 – buffer space.

Regenerator 5 is an independent part of the engine; it is characterized by its own physical and geometric parameters. Buffer space 8 with volume V_b and pressure p_b is borrowed from work [12], but later studies [21] show its frequent negative impact on engine operation. In the future, the buffer space will be excluded from the model, if necessary, by the limit transition $V_b \to \infty$. Thus, the engine will be considered to consist of three main parts: a heater, a cooler and a regenerator. The working piston 1 in the cooler moves freely along the rod 3 of the displacer 2, the latter two are rigidly connected to each other, and one of the ends of the rod with a diameter d_{rod} is attached to a spring 4 with a stiffness coefficient k_d (coefficient of rigidity of the displacer spring). The displacer can move freely inside the cylinder surrounded by a cylindrical regenerator with a length L_r (L_r and A_r – length and area of the working section of the regenerator) and a working space width d_r. When the working piston moves, an electric current is generated by a linear generator; in Fig. 2, the linear generator is not shown, but its feedback on the operation of the machine is taken into account by the damping coefficient D_p. The parameter D_p depends on the generator design and the properties of the electrical load connected to it, but for the steady-state operating mode of the engine with a constant frequency, it can be considered a freely variable parameter [12].

3. Equations of the free-piston Stirling engine model

The regenerator is represented by a narrow and long channel in the space between two coaxial cylinders with diameters d_1 and $d_2 = d_1 + 2d_r$. The average velocity of one-dimensional gas movement in it with density ρ_r and in the direction of the x coordinate is designated u. For cases of flows when the density of the medium changes slightly with pressure, this velocity is found from the equation of conservation of momentum [21]:

$$\frac{\partial u}{\partial t} + u\frac{\partial u}{\partial x} = -\frac{1}{\rho_r}\frac{\partial p}{\partial x} - \frac{1}{8}\cdot\frac{\zeta\Pi}{A_r}|u|u - \frac{1}{2}\delta(x - x_0)K_r|u|u\,. \tag{1}$$

The delta-function $\delta(x - x_0)$ models a sudden change in momentum in a local region folded into a point with coordinate x_0. In typical Stirling machines, the thermal expansion of the gas is small, the pressure also changes little and the compressibility of the gas is insignificant. Therefore, the derivative of the density with respect to time is a small value, compared to convective transfer. As a result, the density ρ_r and the velocity u can only be functions of time. Therefore, instead of (1), we can consider the equation [21]:

$$L_{\mathrm{r}}\frac{du}{dt}=\frac{1}{\rho_{\mathrm{r}}}\Delta p-\frac{1}{8}\zeta\frac{L_{\mathrm{r}}\Pi}{A_{\mathrm{r}}}|u|u-\frac{1}{2}K_{\mathrm{r}}|u|u\,. \tag{2}$$

The pressure difference $\Delta p > 0$ if the gas flows from left to right. For a regenerator (Fig. 2) enclosed in the space between coaxial cylinders, the ratio of the perimeter to the flow area is $\Pi/A_{\mathrm{r}} = 2/d_{\mathrm{r}}$ (height of the working section of the regenerator) (in [21] the erroneous 4 was used instead of 2). The most accurate heater and cooler model should include non-steady-state temperature equations in all parts of the engine [22]. But now the study of the influence of a reversible chemical reaction on the technical characteristics of a free-piston Stirling engine is fundamental. Therefore, the case of constant temperature is considered below, i.e. the isothermal approximation is used [12–14]. The model includes equations of motion of the displacer, piston and gas in the regenerator. The coordinate of the displacer x_{d} with mass m_{d} is measured from the equilibrium position $x_{\mathrm{d},0}$, the initial coordinate of the piston x_{p} with mass m_{p} coincides with the reference point of the coordinate x. The thickness of the piston and displacer is neglected. Thus, there are notations:

– initial position of the piston $x_{\mathrm{p},0} = 0$;

– initial volume of coolant

$$V_{\mathrm{c},0}=\frac{\pi d_1^2}{4}\frac{L_{\mathrm{c},1}+L_{\mathrm{r}}}{2}+\frac{\pi d_2^2}{4}L_{\mathrm{c},2}-A_{\mathrm{rod}}x_{\mathrm{d},0}\,,$$

– cross-sectional area of the rod A_{rod} cross-sectional area of the rod (displacer) and the initial position of the displacer $x_{\mathrm{d},0}$,

$$A_{\mathrm{rod}}=\frac{\pi d_{\mathrm{rod}}^2}{4},\qquad x_{\mathrm{d},0}=\frac{L_{\mathrm{c},1}+L_{\mathrm{r}}}{2}+L_{\mathrm{c},2}\,;$$

– initial volume of heater,

$$V_{\mathrm{e},0}=\frac{\pi d_1^2}{4}\frac{L_{\mathrm{r}}}{2}+\frac{\pi d_2^2}{4}L_{\mathrm{e}}\,.$$

As can be seen, the initial position of the displacer $x_{\mathrm{d},0}$ coincides with the coordinate of the center of the regenerator. The gas in the buffer volume is compressed and expanded under adiabatic conditions with an adiabatic index of γ. The external and initial pressure is denoted by p_0.

The equations of motion of the displacer (taking into account the friction force with the coefficient D_{d}) and the piston have the form

$$m_{\mathrm{d}}\frac{d^2x_{\mathrm{d}}}{dt^2}+D_{\mathrm{d}}\frac{dx_{\mathrm{d}}}{dt}+k_{\mathrm{d}}(x_{\mathrm{d}}-x_{\mathrm{d},0})=p_{\mathrm{b}}A_{\mathrm{rod}}+p_{\mathrm{c}}A_{\mathrm{p}}-p_{\mathrm{e}}A_{\mathrm{d}}\,, \tag{3}$$

$$m_{\mathrm{p}}\frac{d^2x_{\mathrm{p}}}{dt^2}+D_{\mathrm{p}}\frac{dx_{\mathrm{p}}}{dt}=(p_{\mathrm{b}}-p_{\mathrm{c}})A_{\mathrm{p}}\,. \tag{4}$$

The areas of the piston A_{p} cross-sectional area of the working piston, and the displacer A_{d} cross-sectional area of the displacer;

are equal

$$A_{\mathrm{d}}=\frac{\pi d_1^2}{4},\qquad A_{\mathrm{p}}=\frac{\pi(d_1^2-d_{\mathrm{rod}}^2)}{4}\,.$$

Equations (3) and (4) are supplemented by formulas for determining pressures:

$$p_{\mathrm{b}}=p_0\left(\frac{V_{\mathrm{b},0}}{V_{\mathrm{b}}}\right)^{\gamma},\qquad p_{\mathrm{c}}=\frac{R_{\mathrm{g,c}}T_{\mathrm{c}}}{V_{\mathrm{c}}}m_{\mathrm{c}}\,,\qquad p_{\mathrm{e}}=\frac{R_{\mathrm{g,e}}T_{\mathrm{e}}}{V_{\mathrm{e}}}m_{\mathrm{e}}\,. \tag{5}$$

A change in the chemical composition of the gas leads to a change in the gas constant, the gas composition is different in the heater and cooler. Accordingly, two designations are introduced for the gas constant: $R_{\mathrm{g,c}}$ and $R_{\mathrm{g,e}}$. The volumes contained in (5) are found using the formulas

$$V_{\mathrm{c}}=V_{\mathrm{c},0}+A_{\mathrm{p}}(x_{\mathrm{d}}-x_{\mathrm{d},0}-x_{\mathrm{p}}), \tag{6}$$

$$V_{\mathrm{e}}=V_{\mathrm{e},0}-A_{\mathrm{d}}(x_{\mathrm{d}}-x_{\mathrm{d},0}),\qquad V_{\mathrm{b}}=V_{\mathrm{b},0}+A_{\mathrm{rod}}(x_{\mathrm{d}}-x_{\mathrm{d},0})+A_{\mathrm{p}}x_{\mathrm{p}}.$$

The masses of gas in the displacer m_{c} and the heater m_{e} are determined by solving the equations

$$\frac{dm_c}{dt} = -m'_r, \quad \frac{dm_e}{dt} = m'_r. \tag{7}$$

The mass flow rate of gas in the regenerator m'_r is found from equation (2) and this issue is discussed below. The pressure p_r and temperature T_r in the regenerator are taken as the average values in the heater and cooler:

$$p_r = \frac{p_e + p_c}{2}, \quad T_r = \frac{T_e + T_c}{2}. \tag{8}$$

Equalities (8) mean the adoption of a linear dependence on the x coordinate of the change in pressure and temperature in the regenerator. Then the gas density in the regenerator ρ_r is determined from the equation of state

$$\rho_r = \frac{p_r}{T_r R_g}, \tag{9}$$

where the average gas constant R_g is defined as $R_g = (R_{g,c} + R_{g,e})/2$.

Equation (9) is necessary to find the mass of gas in the regenerator m_r. The density ρ_r can be determined more accurately by calculating its average value using the linear functions $p(x)$ and $T(x)$ and the equation of state of the gas for the regenerator [12]. But such averaging, leading to a complex expression, does not provide significant advantages over (9). In Figure 2, between the regenerator and the volumes V_c and V_e, there are local sections of gas flow reversal; they are included in the regenerator and are characterized by the coefficient K_r.

Equation (2) can also be written for the mass flow rate $m'_r(t) = u(t)\rho_r A_r$. Using this definition and taking into account the constancy of the density ρ_r, we write the equation for the flow rate,

$$\frac{dm'_r}{dt} = \frac{A_r}{L_r}\Delta p - \frac{1}{2}\frac{K_\Sigma |m'_r|}{m_r} m'_r, \tag{10}$$

$$K_\Sigma = K_r + \frac{L_r}{2d_r}\zeta, \quad m_r = \rho_r L_r A_r = \rho_r V_r, \quad V_r = L_r A_r. \tag{11}$$

According to Figure 2, the positive direction of gas movement corresponds to the positive sign of the pressure difference Δp, therefore it should be $\Delta p = p_c - p_e$. Since the regenerator is a porous (mesh) structure made of thin metal wire [19, 20], then in the determination of the gas volume V_r in the general case, the porosity should be added as a factor. Porosity should also be taken into account in determining the coefficient ζ. Here it is assumed that the porosity is close to one.

4. Accounting for changes in the composition of the working gas

In volumes V_c and V_e, first-order chemical reactions occur at constant temperatures $T_c = T_{min}$ and $T_e = T_{max}$. In the first of them, the chemical transformation (reverse reaction) occurs according to the scheme B $\rightarrow$ A at a rate of k_c, and in the second (forward reaction) — according to the scheme A $\rightarrow$ B at a rate of k_e. At the same time, a mass of gas enters (or leaves) these volumes at a rate of m'_r. That is, in each of them there can be two sources of substances of types A and B. Each of them in an arbitrary volume has a mass of m_A and m_B, their sum is always equal to the total mass of gas in this volume. Substances A and B are characterized by relative mass concentrations g_A and g_B, their sum is equal to

$$g_A + g_B = 1. \tag{12}$$

For simplicity, the chemical transformation inside the regenerator is not taken into account. The simple relationship (12) between the concentrations allows us to use the equations for only one of them, for example, g_B. The cooler and heater are spatially separated from each other; they differ in the composition of the gas in them. Therefore, the mass concentration g_B will be determined in different ways. Therefore, below g_B is supplemented with indices indicating its value in V_c and V_e, i.e. $g_{B,c}$ and $g_{B,e}$. With their help it is possible to determine the gas constants of the mixture in the cooler $R_{g,c}$ and the heater $R_{g,e}$ [23]:

$$R_{g,c} = R\left(\frac{g_{B,c}}{\mu_B} + \frac{1-g_{B,c}}{\mu_A}\right), \qquad R_{g,e} = R\left(\frac{g_{B,e}}{\mu_B} + \frac{1-g_{B,e}}{\mu_A}\right), \tag{13}$$

where R is the universal gas constant; μ_A, μ_B are the molar masses of substances A and B.

4.1. Chemical reaction in the regenerator

The simplest methods are used to model the chemical reaction in all parts of the engine [27]. In particular, in the volume of the regenerator, the rates of the forward and reverse chemical reactions are approximately equal. Since chemical transformation does not occur in the regenerator as a whole, then when calculating the mass of gas in the regenerator m_r, the gas constant in it $R_{g,r}$ is determined by the conditions:

if $m'_r \geq 0$, then $R_{g,r} = R_{g,c}$; if $m'_r < 0$, then $R_{g,r} = R_{g,e}$.

The mass m_r is found from the equation of state

$$m_r = \frac{p_r V_r}{R_{g,r} T_r}. \tag{14}$$

4.2. Chemical reaction in a cooler

Consider the volume V_c and the **1st case** $m'_r > 0$, then the substance B will decrease due to convective entrainment from this volume and due to the chemical reaction. A simple first-order reaction gives a conservation equation for the mass $m_{B,c}$,

$$\frac{dm_{B,c}}{dt} = -g_{B,c} m'_r - m_c k_c g_{B,c}. \tag{15}$$

By definition of relative mass concentration, $g_{B,c} = m_{B,c}/m_c$. Then, taking into account the first equality in (7), equation (15) can be written for $g_{B,c}$:

$$\frac{dg_{B,c}}{dt} = -k_c g_{B,c}. \tag{16}$$

In the **2nd case** $m'_r < 0$ and the content of gas of type B changes both due to the chemical reaction and due to convective transfer from the heater. In the volume V_e the reaction A $\rightarrow$ B occurs. There its concentration is designated $g_{B,e}$. Now the equation of conservation of mass will take the form

$$\frac{dm_{B,c}}{dt} = -g_{B,e} m'_r - m_c k_c g_{B,c}.$$

After moving here to the concentration $g_{B,c}$, we obtain

$$\frac{dg_{B,c}}{dt} = \frac{g_{B,c} - g_{B,e}}{m_c} m'_r - k_c g_{B,c}. \tag{17}$$

4.3. Chemical reaction in a heater

Here, the chemical reaction is also first order, but now the substance of type B is formed. The equations for concentration are derived in the same way as in the previous example. In the case of $m'_r > 0$, the equation for mass $m_{B,e}$ is obtained

$$\frac{dm_{B,e}}{dt} = g_{B,c} m'_r + m_e k_e (1 - g_{B,e}).$$

To move to the equation for the concentration $g_{B,e}$, we use the second equality in (7) and the definition $g_{B,e} = m_{B,e}/m_e$, as a result this gives

$$\frac{dg_{B,e}}{dt} = \frac{g_{B,c} - g_{B,e}}{m_e} m'_r + k_e (1 - g_{B,e}). \tag{18}$$

In case $m'_r < 0$, the concentration $g_{B,e}$ is determined from the equation

$$\frac{dg_{B,e}}{dt} = k_e (1 - g_{B,e}). \tag{19}$$

5. Simulation results

Equations (3), (4), (7), (10) and (16)–(19) are the main ones. To them are added auxiliary equalities (5), (6), (8), (9), (11)–(14) and formulas for calculating the areas A_p, A_d, A_{rod}, the initial volumes $V_{c,0}$, $V_{e,0}$ and the initial coordinate of the displacer $x_{d,0}$. The choice of initial conditions for the differential equations can be arbitrary, but they should not be physically contradictory. For example, the concentrations $g_{B,e}$ and $g_{B,c}$ can only be within the interval from 0 to 1. The initial masses m_e, m_c and m_r are determined using the equation of state of the gas at a pressure p_0. The initial conditions for the piston and the displacer are

$$x_p(t=0) = \left.\frac{dx_p}{dt}\right|_{t=0} = 0; \quad x_d(t=0) = x_{d,0}, \quad \left.\frac{dx_d}{dt}\right|_{t=0} = 1 \text{ m/s}.$$

The initial velocity for the displacer of 1 m/s is necessary to "start" the engine.

The reversible reaction of formation of nitrogen tetroxide $2NO_2 \leftrightarrow N_2O_4$ is considered [24, 25]. At atmospheric pressure and a temperature of about 150 °C, the working gas consists almost entirely of NO_2, which is brown in color. At a temperature of about 0 °C, the working gas acquires a light-yellow color and consists mainly of N_2O_4. It is assumed here that substance A is nitrogen tetroxide N_2O_4 with a molar mass of $\mu_A = 0.092$ kg·mol^{-1}; substance B is nitrogen oxide NO_2 with a molar mass of $\mu_B = 0.046$ kg·mol^{-1}.

At a low temperature T_c, the predominant (exothermic) reaction of formation of nitrogen tetroxide occurs according to the scheme

$$\mathrm{B} \xrightarrow{k_c} \mathrm{A}.$$

Its thermal effect is 57 kJ/mol. At high temperature T_e, the (endothermic) reaction of formation of nitrogen dioxide occurs according to the scheme

$$\mathrm{A} \xrightarrow{k_e} \mathrm{B}.$$

The efficiency of the equilibrium Stirling cycle with a reversible chemical reaction can be greater than or equal to the efficiency of the equilibrium Carnot cycle with a chemically inert working gas [2]. Cycles with a reversible chemical reaction and having a high efficiency cannot exist at all temperatures of the heater T_{max} and cooler T_{min}. If we combine the condition for the existence of the cycle and for its efficiency to be higher than that of the Carnot cycle for a chemically inert gas, then a restriction on the ratio follows $\Theta = T_{max}/T_{min}$,

$$\alpha_{St} - (\gamma_A - 1)G_1 \le \Theta \le \alpha_{St}, \tag{20}$$

$$\alpha_{St} = \frac{\mu_B(\gamma_B - 1)}{\mu_A(\gamma_A - 1)}, \qquad G_1 = \left(1 - \frac{\mu_A - \mu_B}{\mu_A}\frac{\omega}{\omega - 1}\right)\ln\omega.$$

Inequalities (20) contain the adiabatic indices γ_A and γ_B, as well as the ratio of the volumes $\omega > 1$ of the initial and final states at temperature T_{max}. Since in practice we are limited in the possibilities of choosing substances, the smaller the temperature ratio Θ, the easier it is to create heat engines with an efficiency exceeding that of Carnot engines with a chemically inert working gas.

The heat capacity of NO_2 dioxide at constant pressure is $c_{p,B} = 797$ J·kg^{-1}·K^{-1}(substance B), and that of N_2O_4 tetroxide — $c_{p,A} = 860$ J·kg^{-1}·K^{-1} (substance A) [26]. The adiabatic indices for these gases can be calculated using the formula [22]

$$\gamma = \left(1 - \frac{R}{c_p\mu}\right)^{-1}.$$

Then the adiabatic index of nitrogen dioxide $\gamma_B = 1.294$, nitrogen tetroxide $\gamma_A = 1.118$. Accordingly, the parameter $\alpha_{St} = 1.256 > 1$, which satisfies the condition for obtaining high efficiency [2]. The numerical solution of the equations was carried out by the Runge–Kutta method [27] with the second order of accuracy and with different time steps Δt to check the correctness of the obtained results. The data below were obtained with a step $\Delta t = 10^{-4}$ s.

The engine efficiency was determined as follows: first, the mechanical work powers in the cooler $P_{mech,c}$ and the heater $P_{mech,e}$ are found using the formulas

$$P_{\text{mech, c}} = (p_{\text{c}} - p_0) A_{\text{p}} \left(\frac{dx_{\text{d}}}{dt} - \frac{dx_{\text{p}}}{dt} \right), \qquad P_{\text{mech, e}} = (p_{\text{e}} - p_0) A_{\text{d}} \frac{dx_{\text{d}}}{dt}.$$

These are alternating quantities, but the useful electrical power is produced regardless of the sign of the powers, so their absolute values are used. Therefore, the total power of the mechanical work of the engine P_{mech} is determined by the equation

$$P_{\text{mech}} = \left| P_{\text{mech, c}} \right| + \left| P_{\text{mech, e}} \right|.$$

The electrical power P_{el} is equal to

$$P_{\text{el}} = D_{\text{p}} \left(\frac{dx_{\text{p}}}{dt} \right)^2.$$

Then, averaging over time (this time is equal to several periods of piston oscillations) is performed for P_{mech} and P_{el}, and the ratio is taken as the engine efficiency η_{eng}

$$\eta_{\text{eng}} = \frac{\langle P_{\text{el}} \rangle}{\langle P_{\text{mech}} \rangle},$$

where angle brackets denote time averages.

Inequality (20) is obtained under the assumption that in the section 1→2 (Fig. 1) the concentration g_{A} exactly reaches the value 1, and the value 0 in the section 3→4. However, this is not observed in the simulation, since the heater and cooler constantly exchange mass, and they have finite dimensions. These factors prevent g_{A} from reaching the extreme values 1 and 0. In addition, the Stirling engine cycle differs from the ideal cycle in Fig. 1, b [12], so the conditions for achieving high efficiency η_{eng} may change and not correspond to the predictions [2]. Figures 3–5 are constructed for the following input parameters (Table 1):

Table 1. Parameters of heater, cooler and regenerator.

Heater	Regenerator	Cooler	Buffer space
$m_{\text{d}} = 4.0$ kg; $k_{\text{d}} = 550$ N·m^{-1}; $D_{\text{d}} = 0.94$ kg·s^{-1}; $d_1 = 0.8$ m; $d_2 = 1.1$ m; $L_{\text{e}} = 0.7$ m; $k_{\text{e}} = 9.0$ s^{-1}; $T_{\max} = 383$ K; $x_{\text{d,0}} = 2.73$ m	$d_{\text{r}} = 0.15$ m; $L_{\text{r}} = 1.75$ m; $K_{\text{r}} = 0.05$; $\zeta = 0.06$	$m_{\text{p}} = 3.0$ kg; $D_{\text{p}} = 230$ kg·s^{-1}; $d_{\text{rod}} = 0.05$ m; $L_{\text{c,1}} = 2.0$ m; $L_{\text{c,2}} = 0.85$ m; $k_{\text{c}} = 8.0$ s^{-1}; $T_{\min} = 273$ K	$p_0 = 10^5$ Pa; $\gamma = 1.37$

The buffer volume $V_{\text{b,0}} = 10^5$ m^3, i.e. it is much larger than the volumes of the cooler and heater, so it has virtually no effect on engine operation. The reaction rates k_{c} and k_{e} are selected so that the concentrations of NO_2 and N_2O_4 approximately correspond to the experimental data [25]. The steady-state average powers and efficiencies obtained in the simulation are $\langle P_{\text{el}} \rangle = 13.15$, $\langle P_{\text{mech}} \rangle = 36.28$ kW; $\eta_{\text{eng}} = 0.365$. The oscillation clock frequency $f = 1.56$ Hz.

The average concentration of NO_2 in the cooler $g_{\text{B,c}} = 0.12$, in the heater $g_{\text{B,e}} = 0.67$. The initial changes in concentration over 20 seconds are shown in Fig. 3. If the process in the engine occurred according to the Carnot cycle, the efficiency would be equal to $\eta_{\text{C}} = 1 - T_{\min}/T_{\max} = 1 - 273/383 = 0.287 < \eta_{\text{eng}}$. This result agrees with the conclusion of work [2]. The initial period of engine operation is unstable, the amplitudes of piston and displacer oscillations quickly increase over 12 seconds, but then tend to constant values. But their speeds of movement change greatly in the initial 0.84 seconds, when the working piston shifts to the average position of 0.74 m. The displacer practically remains in the initial position.

Fig. 4 shows the powers P_{mech} and P_{el} only during periods of stable engine operation. Below, the words "stable mode" are applied to large periods of time, when any significant influence of the initial conditions on subsequent engine operation is excluded. Since the pressure p_{c} differs little from the initial value p_0, the thermodynamic cycle in the cooler is shown in Fig. 5 in coordinates (V_{c}; $p_{\text{c}} - p_0$).

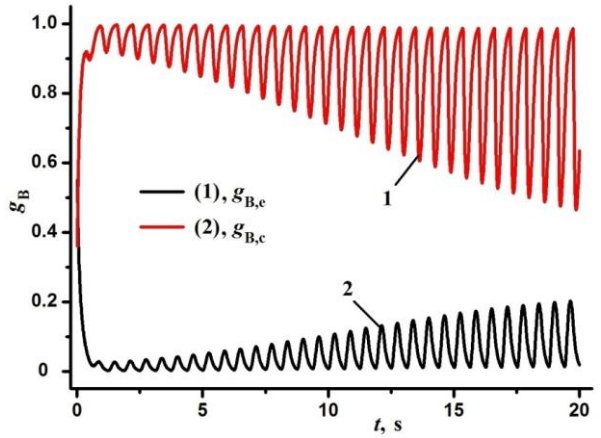

Fig. 3. Changes in the concentration of $g_{B,c}$ and $g_{B,e}$ for 20 s after "launch".

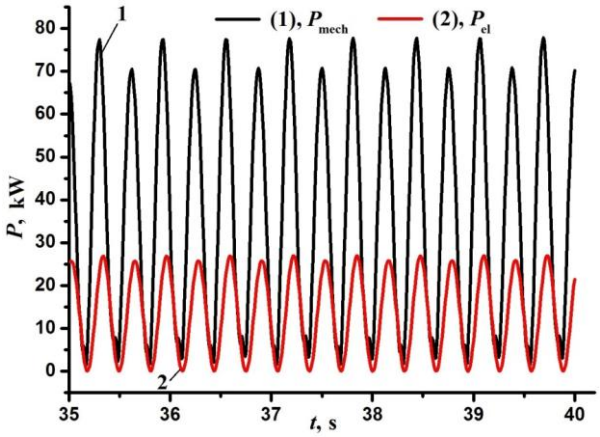

Fig. 4. Changes in powers P_{el} and P_{mech} during averaging time from 35 to 40 s.

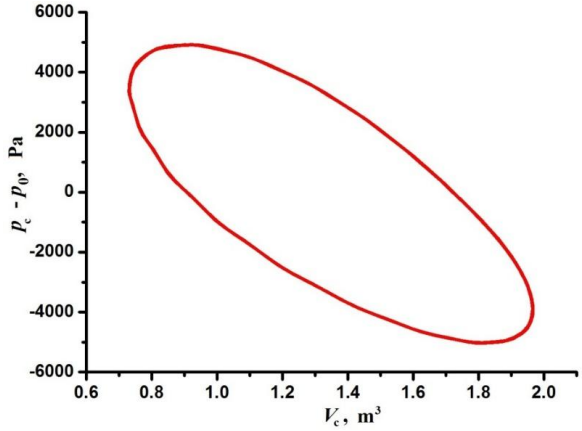

Fig. 5. Representation of the thermodynamic cycle in a Stirling engine with a free working piston. Weak wave-like distortions on the curve are introduced by errors in rounding off the numerical data.

5.1. Operation of a Stirling engine with a chemically inert working gas

Let us consider the operation of the engine without a chemical reaction in the working substance. For this, it is sufficient to take $\mu_A = \mu_B = 0.046$ kg·mol^{-1} in the model; now the working substance consists of one relatively light gas with the same molar mass as nitrogen dioxide gas. Formally, the chemical reaction remains in the model, but it does not lead to physical changes and does not affect the operation of the engine.

Now, stable operation at long times is possible with a lower friction coefficient $D_d = 0.52$ kg·s^{-1} (with the previous $D_p = 230$ kg·s^{-1}). The absence of a change in the molecular weight of the working gas reduced the produced electrical power and efficiency: $\langle P_{el} \rangle = 5.1$, $\langle P_{mech} \rangle = 31.4$ W; $\eta'_{eng} = 0.162$. In addition to the efficiency drop, there was also a strong reduction in the engine's output power; electrical power decreased by 2580 times, mechanical power by 1160 times. Now $\eta_C > \eta'_{eng}$, this result is consistent with the thermodynamics of cycles without a reversible chemical reaction.

5.2. Effect of temperature on the electrical efficiency of the engine

It makes sense to consider noticeable changes in the composition of the working gas in the temperature range from 0 to 170 °C, this is due not only to the peculiarity of the chemical reaction $2NO_2 \leftrightarrow N_2O_4$, but also to the phase state of the working gas [25]. At temperatures below 0 °C, the N_2O_4 gas passes into a liquid state and crystallizes at −11 °C. Therefore, it makes sense to consider the issue of the effect of temperature on the electrical efficiency of the engine with a small change in temperature T_{max} (Table 2).

Together with the temperature T_{max}, the total mechanical power $\langle P_{mech} \rangle$ also increases, which means greater heat consumption from its source. But the rate of growth of the electrical power $\langle P_{el} \rangle$ outpaces it, which is evident from the increase in the efficiency η_{eng}. With the increase in temperature, the amplitude of the oscillations of the displacer and the working piston also increases.

Table 2. Results of the dependence of the main engine parameters on the heater temperature T_{max} at $D_p = 230$ kg·s^{-1}.

№	T_{max}, K (T_{max}, °C)	$\langle P_{el} \rangle$, kW	$\langle P_{mech} \rangle$, kW	η_{eng}
1	363 (90)	10.78	31.29	0.345
2	373 (100)	12.10	33.90	0.357
3	383 (110)	13.15	36.28	0.365
4	393 (120)	14.46	38.71	0.373
5	403 (130)	17.00	44.41	0.383

Therefore, to simulate the operation of the engine at higher temperatures, it is necessary to increase its length to give more freedom of movement to the moving parts of the engine.

6. Production of negative entropy

Erwin Schrödinger [29] explained the ability of biological objects to perform mechanical work as the consumption of negative entropy. However, Schrödinger's position is based only on physical intuition; he did not provide specific examples or models to prove the correctness of his views. In [1, 2], attention is drawn to the similarity between heat engines with a reversible chemical reaction and biological objects. There were two reasons for this: 1) such machines can have very high efficiency with a small difference in temperatures between the heater and the refrigerator; 2) they can exist only in a relatively narrow temperature range. It will be shown below that this analogy is deeper. If the working substance of a heat engine changes its properties as a result of a chemical reaction, then the first law of thermodynamics is written taking into account the chemical work w_{ch} [30]. For example, for the reaction A $\leftrightarrow$ C involving substances A and C with constant heat capacities $c_{\upsilon,A}$ and $c_{\upsilon,C}$ this law can be written as [1]

$$c_\upsilon dT + dw_{ch} + dw = dq\,,$$
$$dw = -pd\upsilon\,, \quad dw_{ch} = (c_{\upsilon,A} - c_{\upsilon,C})Tdg_A\,, \quad c_\upsilon = (c_{\upsilon,A} - c_{\upsilon,C})g_A + c_{\upsilon,C}\,.$$

Now the exergy will contain the sum of mechanical w and chemical work w_{ch}, i.e. $q_{ex} = w + w_{ch}$. The change in chemical work dw_{ch} is determined mainly by the change in the relative mass concentration g_A of substance A. This is sufficient, since the mass concentration g_C of substance C is easily determined through g_A: $g_C = 1 - g_A$. Let us apply Schrödinger's explanation of life to heat engines and thermodynamic cycles. If we consider a biological object as a heat engine, then in an ideal and equilibrium process the entropy q_{in} entering the machine together with heat

$$ds_{in} = \frac{dq_{in}}{T}$$

at temperature T it is partially converted into entropy of exergy

$$ds_{ex} = \frac{dq_{ex}}{T} = \frac{dw}{T} + \frac{dw_{ch}}{T}\,,$$

and the rest

$$d_e s = \frac{dq_{out}}{T}\,,$$

together with heat q_{out} is emitted into the environment. The processes occurring in an ideal heat engine from the point of view of entropy production can be represented by the equality

$$ds_{in} = ds_{ex} + d_e s\,, \quad \text{or,} \quad \frac{dq_{in}}{T} = \frac{dq_{ex}}{T} + \frac{dq_{in}}{T}\,.$$

Integrating over the entire cycle gives

$$\oint \frac{dq_{in}}{T} = \oint \frac{dq_{ex}}{T} + \oint \frac{dq_{out}}{T}\,. \tag{21}$$

The application of equation (21) for the Carnot cycle (Fig. 6) and with a reversible chemical reaction can be written as an equality

$$\frac{q_{\text{in}}}{T_{\max}} = \Delta s_{\text{ex}} + \frac{q_{\text{out}}}{T_{\min}}, \qquad \Delta s_{\text{ex}} = \oint \frac{dq_{\text{ex}}}{T}, \tag{22}$$

где $T_{\min}$ и $T_{\max}$ – минимальная (охладителя) и максимальная (нагревателя) температура.

The Carnot cycle with a reversible chemical reaction is represented in a three-dimensional space of variables s, T and g_{A} (Fig. 6, *a*). In this way it differs fundamentally from the known cycle with a chemically inert working substance.

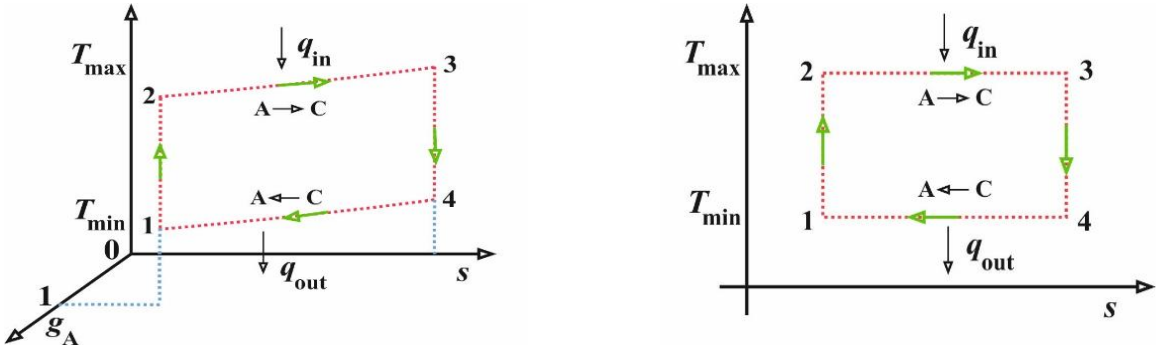

a) *b*)

Fig. 6. Carnot cycle with a reversible chemical reaction in the working substance in s-T-g_{A} coordinates (a) and its projection in s-T coordinates (b).

In (22) $\Delta s_{\text{ex}} = 0$ for a chemically inert working substance, but in the general case equality to zero may not be fulfilled. From (22) the removed heat is determined

$$q_{\text{out}} = \frac{T_{\min}}{T_{\max}} q_{\text{in}} - T_{\min} \Delta s_{\text{ex}}.$$

Using this result for the efficiency of the Carnot cycle η_{C}, the following expressions are obtained

$$\eta_{\tilde{\text{N}}} = 1 - \frac{T_{\min}}{T_{\max}} + \frac{T_{\min}}{q_{\text{in}}} \Delta s_{\text{ex}}, \tag{23}$$

$$\Delta s_{\text{ex}} = \frac{q_{\text{in}}}{T_{\min}} \left(\eta_{\tilde{\text{N}}} - \eta_0\right).$$

Here, for the efficiency of the Carnot cycle with a chemically inert working substance, a separate designation η_0 is introduced,

$$\eta_0 = 1 - \frac{T_{\min}}{T_{\max}}. \tag{24}$$

Thus, in (23), the new cycle is compared with a cycle running on a chemically inert working substance. This is not necessary; any known cycle can be taken as a “reference point”. But the use of such a Carnot cycle with the efficiency (24) turns out to be the most convenient for interpreting subsequent results. Since the exergies of different cycles differ, the index “ex” is not used below, but is replaced by an index indicating a specific cycle. But this does not mean that the entropy under consideration is not related to the exergy. In addition, in order to preserve Schrödinger’s interpretation of the high efficiency of biological objects as a result of consuming negative entropy, the change in entropy taken with a negative sign is further used. For example, for the Carnot cycle $\Delta s_{\text{C}} = -\Delta s_{\text{ex}}$. The efficiency of an ideal Stirling cycle with a reversible chemical reaction η_{St} is determined by the formulas [2]

$$\eta_{\text{St}} = 1 - \frac{T_{\min}}{T_{\max}} G(\omega), \tag{25}$$

$$G(\omega) = \frac{G_{0,1} + G_1}{G_{0,2} + G_1}, \qquad G_1 = \left(1 + \frac{\mu_{\text{C}} - \mu_{\text{A}}}{\mu_{\text{A}}} \frac{\omega}{\omega - 1}\right) \ln \omega,$$

$$G_{0,1} = \frac{1}{\gamma_C - 1}\frac{T_{max}}{T_{min}} - \frac{\mu_C}{\mu_A(\gamma_A - 1)}, \qquad G_{0,2} = \frac{1}{\gamma_C - 1} - \frac{\mu_C}{\mu_A(\gamma_A - 1)}\frac{T_{min}}{T_{max}}.$$

Here, for the expansion coefficients ω_2 and compression coefficients ω_1, their equality is accepted: $\omega_2 = \omega_1 = \omega$. For the change in entropy in the Stirling cycle Δs_{St}, the equality is satisfied

$$\Delta s_{St} = \frac{q_{in}}{T_{min}}\left(\eta_0 - \eta_{St}\right). \tag{26}$$

The supplied q_{in} and removed q_{out} heat are defined as [2]

$$q_{in} = -\frac{R}{\mu_C}T_{max}(G_{0,2} + G_1), \qquad q_{out} = -\frac{R}{\mu_C}T_{min}(G_{0,1} + G_1), \tag{27}$$

$R = 8.31$ J·kg^{-1}·K^{-1}.

The results in Figures 7 (*a*, *b*) based on (25)–(27) were obtained for the expansion coefficient $\omega = 1.1$ and this is a realistic value. At $T_{max} > 340$ K the inequality $\eta_{St} > \eta_0$ is satisfied and at the same time the change in entropy Δs_{St} becomes negative.

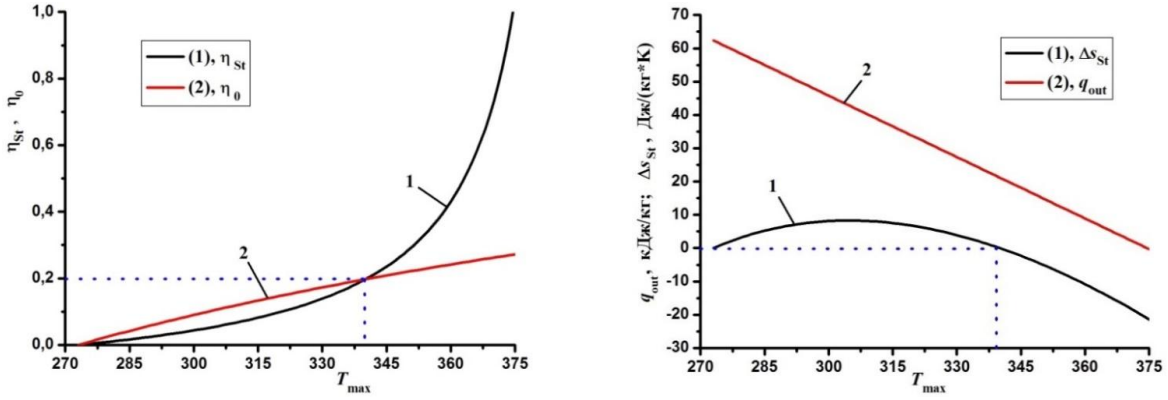

a) *b*)

Fig. 7. Efficiency of the Stirling cycle η_{St} and Carnot η_0 (*a*), as well as changes in entropy Δs_{St} and removed heat q_{in} (*b*) depending on the heater temperature T_{max}.

If we take $\omega = 1.3$, then the inequalities $\eta_{St} > \eta_0$ and $\Delta s_{St} < 0$ are satisfied at the maximum temperature T_{max} of about 330 K. Since the effective flow of the direct reaction $N_2O_4 \rightarrow 2NO_2$ is assumed when obtaining theoretical results (25)–(27), this is possible at pressures below atmospheric. For such pressures, the low-temperature regions in Fig. 7 have a physical meaning. Formula (25) gives overestimated values of the efficiency η_{St} (Fig. 7, a) compared to the simulation data (Table 1). And this difference increases significantly with increasing temperature T_{max}. Most likely, this is due to the influence of friction forces (equations (10) and (11)), as well as the effect of the electrical load, which has a dissipative effect with a coefficient D_d.

7. Conclusion

The conducted modeling showed a higher efficiency of the Stirling engine with a reversible chemical reaction $2NO_2 \leftrightarrow N_2O_4$ compared to the same engine, but with a chemically inert working gas. Moreover, the increase in power when switching from a chemically inert gas to a chemically reacting gas is approximately more than a thousand times, and the efficiency increases by 2.25 times. The obtained modeling results confirm the conclusions made in [1, 2].

A Stirling engine with a free working piston has the property of instability of the initial state; this is evident from the need to give an initial impulse to start it. After this, the oscillations that arise in the engine develop with increasing amplitude until the internal friction forces stop this process. If, in modeling, the friction force is taken as a linear dependence on the speed with a friction coefficient D_d, then its numerical value sometimes has to be selected to obtain a stable engine operating mode.

An increase in power and efficiency is also observed with an increase in the heater temperature. At the same time, due to the increase in the amplitude of oscillations of the working piston, it is necessary to lengthen the engine to obtain higher power and efficiency.

A similar study to the one given above was previously conducted in [27], but where the reaction of methanol formation $CO + 2H_2 \leftrightarrow CH_3OH$ was considered. In this case, the engine power was about 1–1.5 kW with close geometric parameters and temperatures. Thus, the use of the reaction $2NO_2 \leftrightarrow N_2O_4$ is more economically advantageous. Engines with a reversible chemical reaction are similar to biological objects [1, 2], but this conclusion was previously made based on their ability to have high efficiency with a small difference in temperature between the heater and cooler. The ability of such engines to produce negative entropy of E. Schrödinger further confirms the conclusions of [1, 2].

Using the isothermal approximation in the presented model can introduce significant changes to the results obtained above. This can primarily be due to large temperature fluctuations in the heater and cooler. Intensive mass and heat exchange can occur between them due to the regenerator. This can lead to a decrease in the average temperature difference between the heater and cooler. However, this can be minimized by increasing their volumes.

Conflict of interest statement
The authors declare that they have no conflict of interest in relation to this research, whether financial, personal, authorship or otherwise, that could affect the research and its results presented in this paper.

CRediT author statement
Sabdenov, K.O.: Conceptualization, Methodology, Writing-Review & Editing; **Konysbekova, G.K**.: Original Draft, Visualization, Software. The final manuscript was read and approved by all authors;

References

1 Sabdenov K. O. (2021) The thermodynamic Brayton cycle with a reversible chemical reaction. *Tech. Phys*. 66, 1275–1283. https://doi.org/10.1134/S1063784221090164

2 Kanysh Sabdenov. (2023) The Thermodynamics Cycles with a Reversible Chemical Reaction. *Americ. Journ. Modern Phys.*, 12 (2), 14–20. 10.11648/j.ajmp.20231202.11

3 Vialaron, A. (1981). Chemical Storage and Pumping of Solar Energy. In: den Ouden, C. (eds) Thermal Storage of Solar Energy. Springer, Dordrecht., 295–307. https://doi.org/10.1007/978-94-009-8302-1_29

4 Williams O. M. (1980) A comparison of reversible chemical reactions for solar thermochemical power generation. *Revue Phys. Appl.*, 15 (3), 453. https://doi.org/10.1051/rphysap:01980001503045300

5 Egenolf-Jonkmanns B., Bruzzano St., Deerberg G. (2012) Low temperature chemical reaction systems for thermal storage. *Energy Procedia*, 30, 235. https://doi.org/10.1016/j.egypro.2012.11.028

6 Jun Li, T. Zeng, N. (2019) Kobayashi, et all. Lithium Hydroxide Reaction for Low Temperature Chemical Heat Storage: Hydration and Dehydration Reaction. *Energies*, 12(19), 3741. https://doi.org/10.3390/en12193741

7 Chen R, Deng S, Xu W, Zhao L. (2019) A graphic analysis method of electrochemical systems for low-grade heat harvesting from a perspective of thermodynamic cycles. *Energy.* https://doi.org/10.1016/j.energy.2019.116547

8 Ruihua Chen, Weicong Xu, Shuai Deng, Ruikai Zha, Siyoung Q. Choi, Li Zhao. (2023) Towards the Carnot efficiency with a novel electrochemical heat engine based on the Carnot cycle: Thermodynamic considerations. *Energy*, 284, 128577. https://doi.org/10.1016/j.energy.2023.128577

9 Scot T. Martin. Molar. (2025) Heat Capacity for Graphical Pedagogy Applied to Heat Engines, Refrigerators, and Heat Pumps Driven by Chemical Change. *Journal of Physical Chemistry A*., 129 (46), 10762-10770. https://doi.org/10.1021/acs.jpca.5c04285

10 Kovtun I. M., Naumov A. N., Nesterenko V. B. (1967) Stirling cycle on dissociating gas. *Bulletin of the Academy of Sciences of the BSSR, Series of physical and technical sciences* [in Russian]. 1, 52–57. https://www.twirpx.com/file/2561043/

11 Metwally M. M., Walker G. (1977) Stirling engines with a chemically reactive working fluid — some thermodynamic effects. *Journal Eng. Power*. 99 (2), 284–287. https://doi.org/10.1115/1.3446287

12 Langlois, Justin L. R. (2006) Dynamic computer model of a Stirling space nuclear power system. *Trident Scholar project report no. 345*. – Annapolis: US Naval Academy, https://citeseerx.ist.psu.edu/document?repid=rep1&type=pdf&doi=cd482348cc9b1fe3d06ae79d3e5e64f9e78ca0b7

13 Wong H.M, Goh S.Y. (2020) Experimental comparison of sinusoidal motion and non-sinusoidal motion of rise-dwell-fall-dwell in a Stirling engine. *Journ. Mech. Eng., Sci.*, 14 (3), 6971–6981. DOI:10.15282/jmes.14.3.2020.01.0546

14 Snyman H., Harms T., and Strauss J. (2008) Design analysis methods for Stirling engines. *Journal of Energy in Southern Africa*. 19 (13), 4–19. 10.17159/2413-3051/2008/v19i3a3329

15 Salem Ghozzi, R. Boukhanouf. (2015) Computer Modeling of a Novel Mechanical Arrangement of a Free-Piston Stirling Engine. *Journ. Clean Ener. Techn*., 3 (2), 140–144. https://doi:10.7763/JOCET.2015.V3.184

16 Sutapat Kwankaomeng, Banterng Silpsakoolsook, Pongnarin Savangvong. (2014) Investigation on Stability and Performance of a Free-Piston Stirling Engine. *Energy Procedia*., 52, 598–609. DOI: 10.1016/j.egypro.2014.07.115

17 Farid Z. M., Faiz R. M., Rosli A. B. and Kumaran K. (2018) Thermodynamic performance prediction of rhombic-drive beta-configuration Stirling engine. *Ist International Postgraduate Conference on Mechanical Engineering,* https://doi:10.1088/1757-899X/469/1/012048

18 Dovgyallo A. I., Nekrasova S. O., Sarmin D. V., Pulkina A. Yu. (2020) Free piston pulse tube engine: a numerical and experimental power generation estimation. *Journal of Physics: Conference Series*. 1565 (1):012100. https://doi.org/10.1088/1742-6596/1565/1/012100

19 Zhiwen Dai, Chenglong Wang, Dalin Zhang, Wenxi Tian, Suizheng Qiu, G.H. Su. (2021) Design and analysis of a free-piston Stirling engine for space nuclear power reactor. *Nucl. Eng. Techn*., 53 (2), 637–646. https://doi.org/10.1016/j.net.2020.07.011

20 Catapano Fr., Perozziello C., Vaglieco B.M. (2021) Heat transfer of a Stirling engine for waste heat recovery application from internal combustion engines. *Appl. Therm. Eng*., 198, 117492. https://doi.org/10.1016/j.applthermaleng.2021.117492

21 Sabdenov K. O. (2024) A simple model of a Stirling machine (engine) with a free working piston. *Journ. Engin. Phys. Thermoph*, 97 (4), 1034–1041. https://doi.org/10.1007/s10891-024-02974-3

22 Sabdenov K. O., Erzada M., Zholdybaeva G. T. (2024) Simulation of conductions for achieving high electrical power and efficiency in a Stirling engine with a free piston. *Euras. Phys. Techn. Journ.*, 21(4), 49–60. https://doi.org/10.31489/2024No4/49-60

23 Çengel Y. A., Boles M. A., Kanoglu M. (2024) Thermodynamics: An Engineering Approach.10th ed. New York: McGraw-Hill, 948. https://u.eruditor.one/file/3945201/

24 Jones K. (2013) *The Chemistry of Nitrogen: Pergamon Texts in Inorganic Chemistry*. Oxford: Pergamon Press (Elsevier). 242. http://perlego.com/book/4478282/the-chemistry-of-nitrogen-pergamon-texts-in-inorganic-chemistry-pdf , https://doi.org/10.1016/c2013-0-05694-0

25 Kirk-Othmer. (2005) *Encyclopedia of Chemical Technology*. John Wiley Sons. 10, 898. https://www.abebooks.fr/edition-originale/Encyclopedia-Chemical-Technology-Kirk-othmer-John-Wiley/31582420860/bd

26 Bruce E. Poling, John M. Prausnitz, John P. O'Connell. (2001) *The Properties of gases and liquids. Fifth Edition*. McGraw-Hill Companies., 792. Available at: https://www.ebooks.com/en-us/book/300463/the-properties-of-gases-and-liquids-5e/bruce-e-poling/

27 Sabdenov K. O., Smagulov Zh. K., Erzada M., Zhakataev T. A**. (**2025**)** Simulation of a Stirling Engine with a Reversible Reaction CO + 2H2 ↔ CH3OH. *Bulletin of the Karaganda University*: «*Physics Series*»**,** 29(2), 55**–**66. https://doi.org/10.31489/2025ph2/55-66

28 Kalitkin N. N. (2013) *Numerical methods*. Moscow, Academia, 298. [in Russian] https://search.rsl.ru/ru/record/01006711380

29 Rob Phillips, Jane Kondev, Julie Theriot, Hernan Garcia. (2012) *Physical Biology of the Cell*. Garland Science. New York. 1088. https://doi.org/10.1201/9781134111589

30 Reid, Charles E. (1990) *Chemical Thermodynamics*. McGraw-Hill College. 332. https://www.amazon.com/Chemical-Thermodynamics-Charles-Reid/dp/007051769X

AUTHORS' INFORMATION

Sabdenov, Kanysh – Doctor of Phys.-Math. Sciences, Professor, Electrical Engineering Department, Transport and Energy Faculty, L.N. Gumilyov Eurasian National University, Astana, Kazakhstan; https://orcid.org/0009-0008-4733-6667; sabdenovko@yandex.kz

Konysbekova, Gulbarshyn – Master of Technical Sciences, PhD student, Thermal Engineering Department, Transport and Energy Faculty, L.N.Gumilyov Eurasian National University, Astana, Kazakhstan; https://orcid.org/0000-0003-2204-4672 , gulbarshyn_1991@mail.ru; +7-(702)673-00-15